ELSEVIER

Journal of Nuclear Materials 290–293 (2001) 887–891

journal of nuclear materials

www.elsevier.nl/locate/jnucmat

Critical issues in divertor optimisation for ITER–FEAT

A.S. Kukushkin [a,*], G. Janeschitz [a], A. Loarte [b], H.D. Pacher [c], D. Coster [d], D. Reiter [e], R. Schneider [f]

[a] *ITER JCT, Garching JWS, Boltzmannstrasse 2, D-85748 Garching, Germany*
[b] *EFDA, Close Support Unit, Garching, Germany*
[c] *INRS-Energie et Matériaux, Varennes, Québec, Canada*
[d] *Max-Planck-Institut für Plasmaphysik, Garching, Germany*
[e] *FZ Jülich, Jülich, Germany*
[f] *Max-Planck-Institut für Plasmaphysik, Greifswald, Germany*

Abstract

A strong effect of the shape of the divertor floor near the separatrix strike point on power loading of the divertor targets in ITER–FEAT is found in the modelling studies. A similar effect has been demonstrated in JET experiments with Mark I and Mark II divertors (A. Loarte, Nucl. Fusion 38 (1998) 587; R. Monk, et al., in: Proceedings of the 24th EPS Conference on Controlled Fusion and Plasma Physics, Berchtesgaden, 1997, vol. 21A, p. 117) thus providing experimental verification of the modelling results. An operational window in six-dimensional phase space is found and different controls, like pumping speed or impurity seeding, are considered for ITER–FEAT.

Keywords: 2D model; B2/EIRENE; Divertor; Geometry effect; ITER; Particle control; Plasma modelling; Power exhaust; Target plate

1. Introduction

Divertor optimisation is performed using the B2-Eirene code package [1,2], verified as far as possible against experiment. The plasma consists of DT, He, and C ions, with or without Ne seeding, with one fluid per charge state and the same modelling conditions as those in [3,4].

2. Effect of divertor geometry

Design studies undertaken in the last two years to reduce the cost (i.e., size and performance) of ITER have resulted in a device called ITER–FEAT [5]. During these studies, the divertor geometry was varied widely but the vertical target plates were retained. Although some modelling runs [6] showed a significant impact of the divertor geometry on the peak power loading of the targets and on the conditions for helium pumping, no clear trends were seen in other cases. Therefore, parameters and design features other than those that were varied deliberately (length, angle, baffling, etc.) are critical in determining the response of the plasma to a geometry variation. The configuration of the divertor floor at the intersection with the vertical target (more or less pronounced 'V' shape) and its position with respect to the separatrix strike point, varied in the course of this modelling, could be such a feature, producing plasma plugging and/or modifying impurity transport.

A tight corner near the strike-point can be plugged by the plasma, and the neutrals accumulate there until a partial detachment occurs, thereby reducing the power load near the strike point. JET experiments with Mark I and Mark II divertors for which the separatrix was swept across the vertical and horizontal targets [7,8] also support this picture. When the strike point moves across

* Corresponding author. Tel.: +49-89 3299 4122; fax: +49-89 3299 4165.
E-mail address: kukusha@itereu.de (A.S. Kukushkin).

0022-3115/01/$ - see front matter
PII: S0022-3115(00)00457-8

the horizontal target or the plasma density is low (weak plasma plugging of neutrals), the profiles of ion saturation current, I_{sat}, measured by probes embedded in the target do not change. However, at high density, I_{sat} is reduced around the strike point for probes near the corner – a signature of partial detachment. The H_α measurements indicate a drastic increase of the neutral density in the divertor corner when the plasma density increases, and earlier modelling for JET reveals a strong recombination near the divertor corner [9].

The effect of the target geometry could also be related to the impurity transport. If the inner leg of the 'V' becomes a part of the target, i.e., receives considerable ion flux in addition to neutrals, the flux pattern of impurity neutrals produced at the target due to either recombination or sputtering can be modified, directing the flux toward the upstream region of hotter plasma. This can increase the radiation efficiency and reduce the power reaching the targets.

To distinguish plasma plugging and impurity transport effects, two minor modifications of the ITER–FEAT divertor were considered (Fig. 1). The first one, 'V-out', employs a short wall just inside the private flux region (PFR) shielded by the dome. While helping to confine the neutrals in the vicinity of the strike point, this short wall does not affect the carbon atom transport. We assume full absorption of carbon particles on all the material surfaces and carbon sputtering on the targets only. The second configuration, 'V-in', includes a dump target from which the carbon atoms are sputtered, and which directly affects their flow. As will be shown below (Section 3.4 and Fig. 5), the peak power load at the same upstream density for both V shapes is lower by about 30% than that of the straight target, and there are only minor differences between V-in and V-out. Therefore, improved neutral retention is concluded to be the dominant mechanism responsible for the reduction of the peak power load.

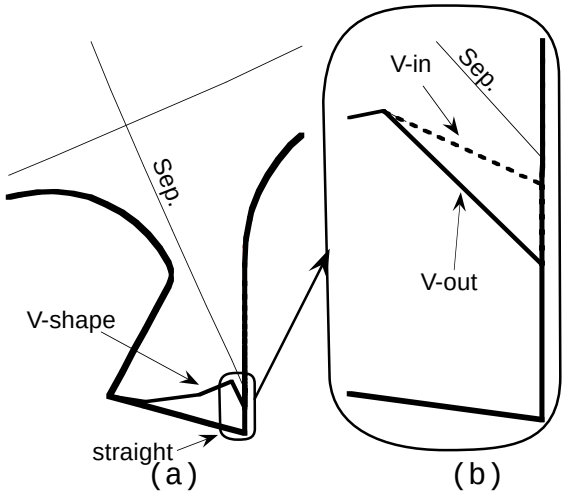

Fig. 1. Model divertor geometry of ITER–FEAT (a) and two V-shape variants (detail in b).

3. Operational window

The window for divertor operation in ITER is delimited by several constraints arising from core plasma and technology requirements [5].

First, the divertor plasma must be compatible with core plasma conditions ensuring the necessary reactor performance, as given by the core plasma modelling for ITER. The upstream plasma density at the separatrix, n_s, which is the edge density for the core plasma, must be limited to 3.3×10^{19} m^{-3}, one-third the core density. The helium concentration in the core, c_{He}, is limited by fuel dilution. Z_{eff} at the core is limited by the acceptable impurity radiation. The plasma flow Γ_{core} from the core across the core-edge interface (CEI) is limited to $\Gamma_{core} \geqslant 0$ since DT burn-up (small) is the only sink of ions inside the separatrix. Note that we take the values of c_{He} and Z_{eff} at the CEI, approximately 5 cm inside the separatrix, as representative for the core plasma. We specify the plasma density at the CEI as the boundary condition, and calculate Γ_{core}.

Secondly, the plasma parameters must be compatible with various technological requirements. The peak power on the targets, q_{pk}, must be below a certain value to satisfy constraints on the plasma-facing components. The particle throughput, Γ_{DT}, is limited by the capacity of the pumping and tritium processing facilities and tritium inventory considerations. Γ_{core} is limited above by the capacity of the core fuelling system (pellet injection, neutral beams). Other constraints could arise from wall and target erosion and safety considerations but these are not considered yet.

The limits of this six-dimensional operational window are given in Table 1. Different means to control the divertor operation are used to explore the window. The gas puffing rate is kept constant at 110 Pa m^3/s in the present calculations. The core fuelling varies when we change the plasma density at the CEI. The pumping speed, S_p, is kept approximately constant in the density

Table 1
Limits of the operational window of the ITER–FEAT divertor

Peak power load on the targets	$q_{pk} \leqslant 10$ MW/m^2
DT particle throughput	$\Gamma_{DT} \leqslant 200$ Pa m^3/s
Core fuelling	$0 \leqslant \Gamma_{core} \leqslant 100$ Pa m^3/s
Upstream plasma density	$n_s \leqslant 0.33 \times 10^{20}$ m^{-3}
Helium concentration in the core plasma	$c_{He} \leqslant 0.06$
Z_{eff} in the core plasma	$Z_{eff} \leqslant 1.6$

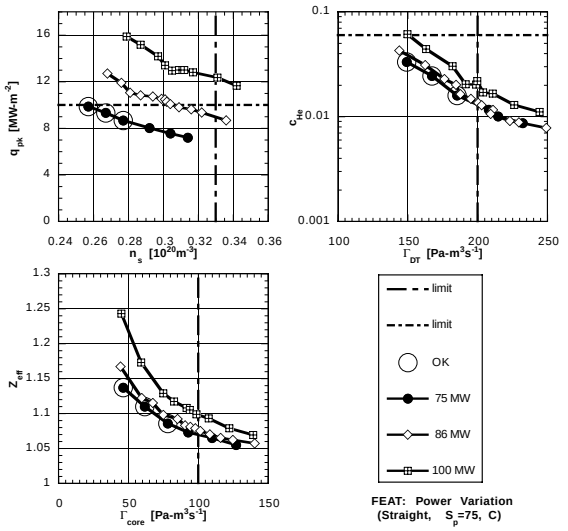

Fig. 2. Three views of the 6D operational window for the ITER–FEAT divertor. Straight vertical target configuration, $S_p = 75$ m^3/s, no neon seeding, three levels of input power. Points within the 6D window are circled.

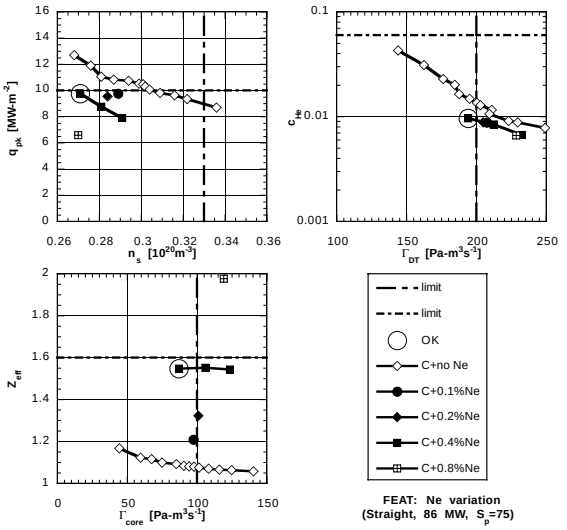

Fig. 3. Same views as Fig. 2, but with neon seeding, $P_{in} = 86$ MW.

scans and varied between scans. Impurity seeding, presently neon, is used to explore the margins in Z_{eff}. Input power, P_{in}, depends on the plasma core conditions and is varied from 75 MW ($P_{fusion} = 410$ MW, $Q = 10$, 40% core radiation) to 86 MW ($P_{fusion} = 410$ MW, $Q = 10$, 30% core radiation) and to 100 MW ($P_{fusion} = 600$ MW, $Q = 24$, 30% core radiation, or $Q = 13$, 40% core radiation), the He production rate is consistent with the fusion power. The divertor geometry is also varied to optimise the window.

3.1. Power variation

Initially, we consider density scans for various input powers for the original ITER–FEAT divertor with straight targets, Fig. 1, with the full pumping speed of 75 m^3/s and no impurities other than carbon and helium. The 6D (q_{pk}, n_s, Z_{eff}, Γ_{core}, c_{He}, Γ_{DT}) operating window is shown in Fig. 2. Operational points inside the 6D window are seen to exist only at 75 MW. At higher powers, 86 MW and above, whenever the peak power load is brought low enough the particle throughput and eventually the upstream density become too high. However, there is a considerable margin in Z_{eff} and some margin in c_{He}.

3.2. Neon seeding

To exploit the margin in Z_{eff}, we introduce some neon seeding in addition to the naturally sputtered carbon (Fig. 3). There is now one point in the window for 86 MW, but it is practically at the corner, almost limited by all the q_{pk}, Z_{eff}, and Γ_{DT}. There is therefore not much room for optimisation in this direction. Note that in this case, neon largely replaces carbon as the radiator, radiating further away and thereby reducing the peak heat load, but producing higher Z_{eff}. Indeed, when the neon radiation becomes significant, the power left for hydrogen recycling decreases, decreasing the ion flow to the target which produces the sputtered carbon. Seeding with a different impurity having a radiation efficiency higher than carbon could be more effective – the trade-off here is between radiated power and Z_{eff}.

3.3. Reduction of the pumping speed

To tradeoff the margin in c_{He} against throughput, one can reduce the pumping speed to reduce the throughput while keeping the same neutral density in the divertor (Fig. 4). This reduction opens the window for 86 and 100 MW. Reducing the pumping speed leads to higher c_{He} at the same upstream density, but somewhat lower c_{He} at the same throughput. A combination of neon seeding with the reduction of S_p works as it did for the higher S_p, yielding some 20% reduction of q_{pk}.

3.4. Variation of the divertor geometry

To optimise the operating window, the V-shapes and the straight target have been compared (Fig. 5). At high S_p, 75 m^3/s, the V-shaped geometries show much better performance than the straight one: q_{pk} at the same upstream density for both V shapes is lower by about 30%

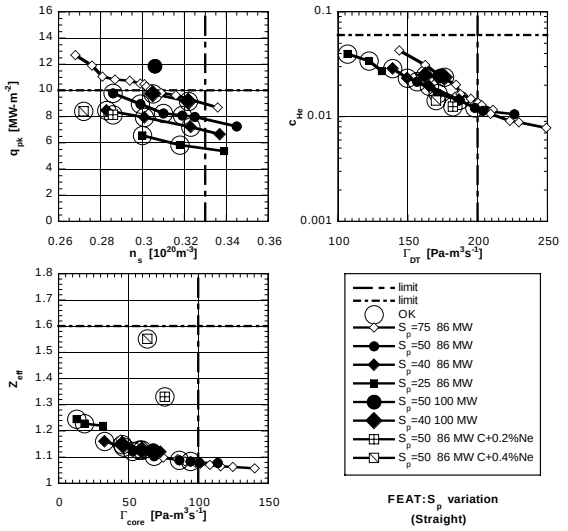

Fig. 4. Same views as Fig. 2, but different pumping speeds ($S_p = 75$, 50, 40, and 25 m^3/s), $P_{in} = 86$ and 100 MW. Two points with reduced pumping speeds and neon seeding are also shown.

than that for the straight target, with the V-in configuration slightly better. For the V configurations, the 100 MW curve lies at the corner of the window in q_{pk} and Γ_{DT}, and the 86 MW points investigated lie just outside the Γ_{DT} limit implying that acceptable solutions exist at this power at somewhat lower n_s. A reduction of the pumping speed should then increase the available operational space, and the margin in Z_{eff} suggests that impurity seeding can also be used here. Note that helium removal does not deteriorate with our V-shaped target configurations.

4. Conclusions and discussion

A V-shaped configuration of the target and divertor floor is beneficial for divertor performance. It provides a considerable reduction of the peak power loads on the target without adversely affecting the helium removal. The effect is mostly due to accumulation of neutrals near the strike point when the V is plugged by plasma, as confirmed by the available experimental data from JET. Such a configuration could also be useful for transients such as ELMs, providing some shielding for the targets. However, it can negatively affect the operational flexibility of the machine by reducing the freedom of positioning the strike point. On balance, as a result of these studies, it is recommended to provide a V-shaped target configuration in ITER–FEAT.

An operational window in six-dimensional phase space for ITER–FEAT is shown in Fig. 6. Only points which satisfy all the constraints and which are produced using the different means of divertor operation control discussed above are shown, demonstrating that powers up to 100 MW can be accommodated. Variation of the pumping speed and fuelling rate in combination with impurity seeding provides control of the operational point within the window; a further exploration of these control means is in progress.

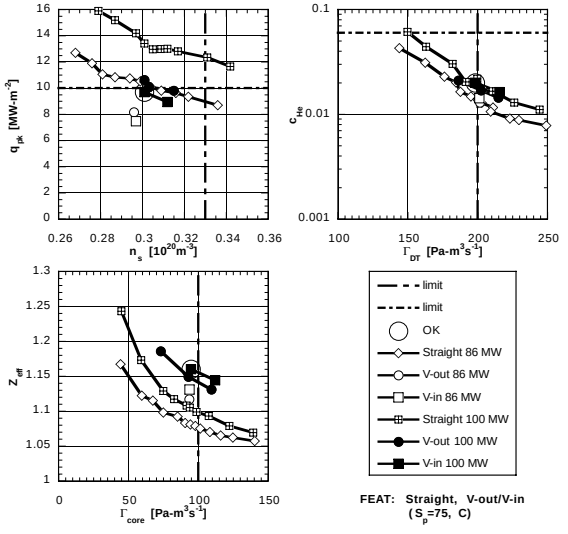

Fig. 5. Same views as Fig. 2 for variations of ITER–FEAT (straight vertical target vs. V-shape), $S_p = 75$ m^3/s, no neon seeding, $P_{in} = 86$ and 100 MW.

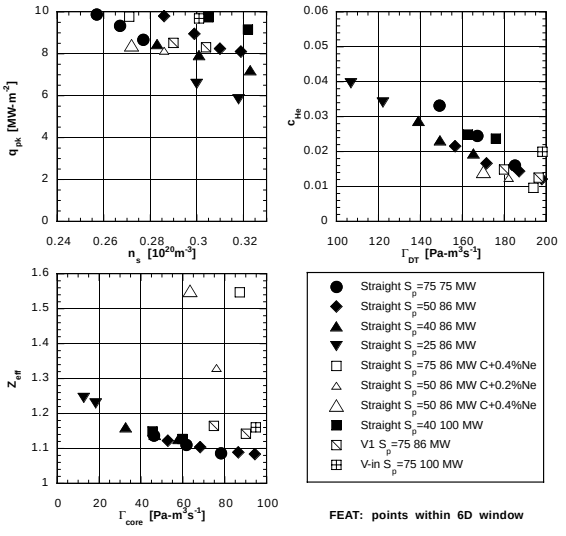

Fig. 6. The 6D operational window – summary. Only acceptable points within window are shown.

Acknowledgements

This report is an account of work undertaken within the framework of the ITER EDA Agreement. The views and opinions expressed herein do not necessarily reflect those of the Parties to the ITER Agreement, the IAEA or any agency thereof. Dissemination of the information in this paper is governed by the applicable terms of the ITER EDA Agreement.

References

[1] D. Reiter, H. Kever, G.H. Wolf et al., Plasma Phys. Control Fus. 33 (1991) 1579.
[2] R. Schneider, D. Reiter, H.-P. Zehrfeld et al., J. Nucl. Mater. 196–198 (1992) 810.
[3] H.D. Pacher, A.S. Kukushkin, D.P. Coster et al., J. Nucl. Mater. 266–269 (1999) 1172.
[4] A.S. Kukushkin, H.D. Pacher, D.P. Coster et al., Fusion energy 1998, in: Proceedings of the 17th Conference, Yokohama, 1998, IAEA, Vienna, 1999, p. 1013.
[5] G. Janeschitz et al., these Proceedings, p. 1.
[6] A.S. Kukushkin et al., in: Proceedings of the 26th EPS Conference on Controlled Fusion and Plasma Physics, Maastricht, 1999, paper P4.046.
[7] A. Loarte, Nucl. Fus. 38 (1998) 587.
[8] R. Monk et al., in: Proceedings of the 24th EPS Conference Controlled Fusion Plasma and Physics, Berchtesgaden, vol. 21A, 1997, p. 117.
[9] K. Borrass et al., in: Proceedings of the 24th EPS Conference Controlled Fusion Plasma and Physics, Berchtesgaden, vol. 21A, 1997, p. 1461.